JAES | JOURNAL OF APPLIED ENGINEERING SCIENCE | www.engineeringscience.rs
ISTRAŽIVANJA I PROJEKTOVANJA ZA PRIVREDU

Indexed by

DERRICK CRANE ROBUSTNESS SCENARIOS

Claudio Bernuzzi
Department of Architecture, Built environment and Construction engineering (ABC), Politecnico di Milano, Milano, Italy

Elisa Bertinotti
Structural Engineer, Milan, Italy

Massimo Frau
Structural Engineer, Milan, Italy

Marco Simoncelli
Department of Architecture, Built environment and Construction engineering (ABC), Politecnico di Milano, Milano, Italy

Key words: *derrick crane; steel angle; warping torsion; robustness analysis; localized damag*
doi:10.5937/jaes0-34255

Cite article:

Bernuzzi C., Bertinotti E., Frau F., Simoncelli M. (2022) DERRICK CRANE ROBUSTNESS SCENARIOS, *Journal of Applied Engineering Science*, 20(2), 523 - 536, DOI:10.5937/ jaes0-34255

Online aceess *of full paper is available at: www.engineeringscience.rs/browse-issues*

Istraživanja i projektovanja za privredu
Journal of Applied Engineering Science

Original Scientific Paper

doi:10.5937/jaes0-34255

Paper number: 20(2022)2, 958, 523-536

DERRICK CRANE ROBUSTNESS SCENARIOS

Claudio Bernuzzi[1,]*, Elisa Bertinotti[2], Massimo Frau[2], Marco Simoncelli[1]
[1]Department of Architecture, Built environment and Construction engineering (ABC), Politecnico di Milano, Milano, Italy
[2]Structural Engineer, Milan, Italy

The paper deals with derrick cranes (derricks) that are equipment typically used in the mining industry and focuses on the analysis of few robustness scenarios. Derricks are composed of built-up steel members which are widely and efficiently used in hoisting applications due to their high payloads at relevant outreaches. During the in-service use, local damages might occur and as such, the aim of the paper is to study how such damages influence the overall structural performance. In particular, reference was made to a derrick for which six geometrical configurations and five different damage scenarios have been analysed. Owing it to the extensive use of angles in the built-up component of each derrick, structural analyses have been carried out by using a commercial refined finite element analysis package (FEAP) offering the warping torsion as an additional degree of freedom for each beam node. Research outcomes allow for a clear identification of the parts of a derrick that should be protected and well-designed to guarantee a robust structure for its entire in-service life.

Key words: derrick crane; steel angle; warping torsion; robustness analysis; localized damag

INTRODUCTION

Due to the high payloads that can be guaranteed at relevant outreaches, built-up steel members [1] are extensively used to realize many types of lifting devices, such as overhead and gantry cranes, jibs of mobile cranes, portal cranes, tower and derricks cranes. The last ones (simply identified in the following as derricks), which are the focus of this paper, are generally used in marine, material handling fields and the mining sector. From a structural standpoint, derricks are stationary cranes whose masts are supported by two rigid inclined legs called tie rods (Figure 1).

Figure 1: A typical derrick used in quarries

Derricks are equipped with three distinct mechanical components (Figure 2), each allowing one movement: tower and boom rotation in the horizontal plane, the luffing of boom in the vertical plane and the lifting of the load. The tower bottom, where engines and drums are located, is connected to the ground by means of a slewing wheel allowing for the rotation of the tower together with the boom. The boom moves in the vertical plane by means of a system of ropes running from the tower base to its top and ending at the boom tip. Due to the national limits for transportation via trucks, the structural components are steel modular members prepared in shops of appropriate geometry, moved via trucks and assembled in-situ via bolted splices. As stationary equipment, derrick bases are restrained on a reinforced concrete foundation or directly fixed to the rock in three points, i.e. at tower base and at the tie-rods bases. Derricks usually stay assembled in the same place for many years: in mining sector, the cultivation of a single plane in a quarry may last as long as 15 to 20 years, sometimes longer. This involves many problems related to possible damages induced by fatigue, stability of anchorage points over time, effects of environmental actions on structures and corrosion. Moreover, damages may be difficult to detect, as several points in these structures are not easy to access while derricks are in service.

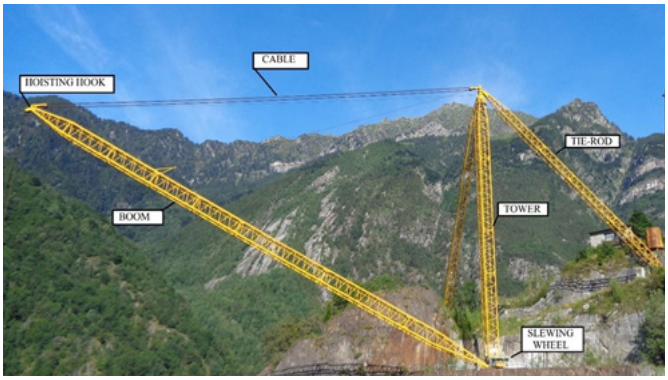

Figure 2: Main components of stiffleg derrick

*claudio.bernuzzi@polimi.it

In European countries, in compliance with Machinery Directive [2], derricks must be equipped with several controls and limit switches to prevent overloading, over speeding and overtravel. Human factors play an important role in safety [3]: designers cannot foresee every possible improper use of a crane, so a great way to mitigate risk is training, knowledge and the skill of riggers and crane users. Accidents are mainly the result of a combination of actions and causes. Wrong proceedings, usage with low visibility [4], unfavourable environmental conditions and tampering with safety devices are all actions that together with the lack of maintenance, mistakes in design and errors in installation may lead to accidents, ruptures and even collapse. There are a few researchers that have recently addressed the failure analysis of these structures, mainly investigating the influence of thermal excursion on cranes behaviour [5] as well as fatigue life of the K-type welded connections [6]. The study of wind effects and a correct estimation of dynamic behaviour are also of fundamental importance in designing safe cranes ([7] to [9]). Furthermore, Solazzi et al. ([10] to [12]) studied the dynamic effects on derricks induced by sudden load releases by using finite element analysis packages (FEAPs); attention has been mainly focused on the buckling phenomena as well which are, in many cases, responsible for the boom collapse. In general, the outcomes associated with these studies are based on refined FE solid/shell models, which give very accurate results but always appear as very expensive for the mesh generation time as well as for the required expertise. In a few cases, numerical design parameters derive from FE analyses carried out by using the traditional 6 degree of freedom (DOFs) beam finite element models. Owing to the presence of mono-symmetric cross-section members, the use of these FE elements could lead to an inaccurate appraisal of the structural response, as stated in [13], where different derricks have been analysed also by considering 7 DOF beam formulation, i.e. including the cross-section warping as additional 7th DOF, necessary to fully capture all the effects associated with warping torsion. As of now, no attention has been paid to the robustness of derricks, which is the focus of this paper. As well-established in literature [14], robustness is a desirable property of structural systems which mitigates their susceptibility to progressive collapse or disproportionate damage. In a robust structure, local damage of a small element will not bring overall structural collapse. As derricks have to guarantee in-situ full efficiency for a period generally greater than 15-20 years, corrosion could affect main structural components, reducing member resistance [15] up to the overall collapses. Furthermore, failures can also be due to a local damage including: i) one of the members of a derrick reaches the maximum load carrying capacity and collapse and ii) an accidental impact on the structure, and, in particular, on a tie-rod bases, as these are the only zones connected directly to the ground. While the probability of the latter happening is very low, the former is more frequent (Figure 3) and hence why it is of great and practical interest. In the present paper, a direct approach has been adopted to study derrick robustness. Reference is made to a typical derrick considered in 6 different geometrical configurations. For each of them, the most highly stressed elements as well as those having the highest probability to be subjected to the spread of corrosion have been identified. Then, these elements were removed from the initial model and new design analyses were carried out to re-evaluate the safety of all the components. Differences between the typical design parameters associated with both undamaged and damaged conditions were carefully considered using for the numerical analyses 7DOFs FE beam elements.

Figure 3: Overall structural collapse due to local damage in a derrick crane

DERRICK DESIGN FEATURES

As far as derrick design provisions are concerned, it is worth noting that while in the U.S., ASME issued the first Code of Safety Standards specific for cranes in 1916 and in Germany DIN 120 cranes code was originally published as late as 1936: this code coupled with the FEM series became the reference point for European crane designers and manufacturing engineers for a few decades. Since the records of using these standards are mainly positive and satisfactory, basic principles changed only a little over the years. Anyways, about a decade ago, UNI EN13001 set the current crane design standard adopted in Europe. A different view has been introduced in respect to previous FEM and DIN standards. As is known by many, limit state design has in fact substituted the allowable stress method for structural design in many European countries along with some others. The amplification coefficients of former DIN 15018 [16] and FEM 1.001 [17] are often used: these standards, addressed to lifting equipment design, have been widely used until a few years ago and their contents have been included in the European design reference that now has to be considered [18]. In this chapter, few remarks on the key features of mono-symmetric cross-section members (i.e. angles) are proposed (§2.1) together with the design approach (§2.2) that was adopted for the practical cases herein discussed.

As to the Bimoment influence on the global behaviour

As already mentioned, the most commonly used commercial FE analysis packages (FEAPs) offer only a beam element characterized by 6 DOFs per node. This classic formulation is adequate to capture the response of only bi-symmetric cross-section members, i.e. the one characterized by the coincidence between the shear center and the cross-section centroid. As already discussed with reference to derricks [13], in case of built-up elements composed by angles. It is necessary to use the so-called 7DOFs FE beam formulation. In particular, the warping of the cross-section (θ) is considered as this additional DOF, the 7th, which is defined on the basis of the torsional rotation (φx), as:

$$\theta = \theta(x) = -\frac{d\varphi_x}{dx} \tag{1}$$

Few FEAPs offering the 7DOFs beam formulation, based on the well-established Vlasov theory, are available in the market. Numerical analyses herein considered have been carried out via the commercial ConSteel software [19], which is characterized by a strong and robust theoretical background and has been extensively validated by authors with several benchmarks. As far as angles are concerned, a key aspect is represented by the evaluation of the warping constant Iw of the cross-section, defined as:

$$I_w = \int \omega^2 dA \tag{2}$$

where ω is the sectorial area evaluated with respect to the shear center. In profiles with plates whose mid-line converges at the same point (L, T and X cross-sections), the location of the shear center is at the intersection of the center lines of the legs. Consequently, if only the distribution of the sectorial area at the midline is considered, the warping constant is nil. However, this approximation is not correct, especially for angles [20] neglecting the variability of the warping along the thickness of the cross-section (Figure 3). As depicted in the figure, it is possible to take into account the effective distribution of the sectorial area.

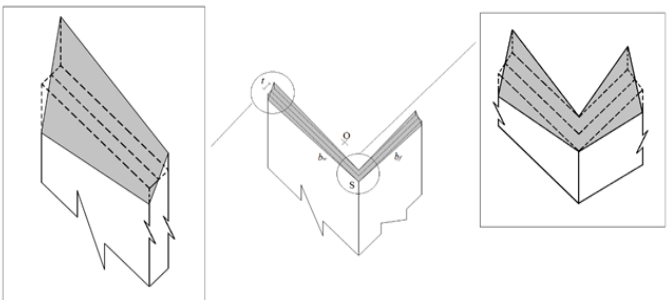

Figure 4: Warping deformation of an angle

With reference to an angle with the legs bf and bw (with bf <bw) and thickness t, according to [21] the maximum sectorial area is:

$$\omega_{max} = b_w \frac{t}{2} \tag{3}$$

The sectorial area starts from zero and varies linearly with the length, by applying eq. 2) to this distribution (depicted in Figure 3), warping constant can be defined as:

$$I_w = \frac{t^3}{36}(b_f^3 + b_w^3) \tag{4}$$

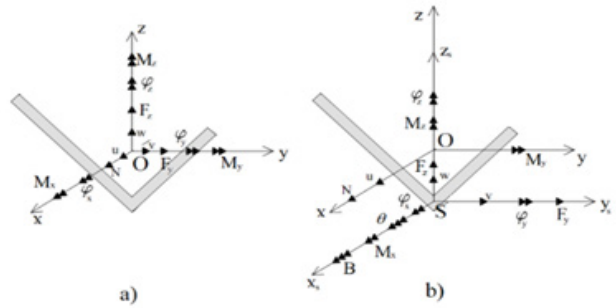

Figure 5: a) six and b) seven DOFs FE beam formulations

In case of a 6DOFs beam element the generalized displacements are wrongly referred only to the centroid (O) which is considered coincident with the shear center (S), as in Fig. 4a. Indeed, in angles as well as in other mono-symmetric cross-sections, generalized displacements must be referred to the shear center (Fig. 4b) with the only exception of the axial displacement u which is related to the centroid. Like in traditional 6DOFs formulation, bending moments (M_y and M_z) and axial force (N) are referred to point O, while bimoment (B), shear forces (F_y and F_z) and uniform torsion moment (Mx) are related to point S. The main point of this beam element formulation is that axial force, bending moments and bimoment and shear actions significantly contribute to the geometric stiffness (i.e. contribution on the buckling and second order results). Furthermore, these terms strictly depend on the distance between load application point and shear center as well: this, in case of bi-symmetric cross-section members, is nil. In structural systems having mono-symmetric cross-section profiles, buckling load estimation and accurate second order analysis require the definition of all the Wagner constant in the geometric stiffness matrix [21].

Derrick design via the General Method

The General Method (EC3-GEM) is a well-established design approach proposed in the EN1993-1-1 [22], appropriate also for structural components having complex support conditions or non-standard geometric configurations [23]. According to GEM, safety of members (SI) is guaranteed when:

$$SI = \frac{\gamma_M}{\chi_{op}\alpha_{ult.k}} \leq 1 \tag{5}$$

where χ_{op} is the global buckling reduction factor associated to the overall system, $\alpha_{ult,k}$ is the minimum load multiplier, i.e. the one associated with highly stressed cross-section and γ_M is the material safety factor.

In the more general case of bi-axial bending of mono-symmetric cross-section members, the ultimate load multiplier for resistance, $\alpha_{ult,k}$ is determined as:

$$\frac{1}{\alpha_{ult,k}} = \frac{N_{Ed}}{A \cdot f_y} + \frac{M_{y,Ed}}{W_{el,y} \cdot f_y} + \frac{M_{z,Ed}}{W_{el,z} \cdot f_y} + \frac{B_{Ed}}{B_{Rk}} \quad (6)$$

where A is the cross sectional area and W_{el},y and $W_{el,z}$ are the flexural moduli of the cross-section along the principal axes. Bimoment resistance B_{Rk}, which can be appraised only the variability of the warping along the angle thickness is considered (Figure 3), is defined as:

$$B_{Rk} = \frac{I_w}{\omega_{max}} f_y \quad (7)$$

where I_w is calculated in according to eq. 4) and ω_{max} is the maximum sectorial area. The global slenderness of the whole structure $\overline{\lambda_{op}}$ is defined as:

$$\overline{\lambda_{op}} = \sqrt{\frac{\alpha_{ult,k}}{\alpha_{cr}}} \quad (8)$$

α_{cr} being the first critical elastic buckling load multiplier, that can be different in terms of value and buckling mode, between the selected beam formulation. Therefore, the reduction factor χ_{op} is defined as:

$$\chi_{op} = \frac{1}{\phi_{op} + \sqrt{\phi_{op}^2 + \overline{\lambda_{op}}^2}} \quad (9)$$

being φ_{op} equal to:

$$\phi_{op} = 0.5\left[1 + 0.34(\overline{\lambda_{op}} - 0.2) + \overline{\lambda_{op}}^2\right] \quad (10)$$

THE CONSIDERED CASES

The numerical phase of this study has been referring to an existing derrick (Figure 4), installed in a marble quarry on the Italian Alps. Boom length is 70 m, tower height is 40 m and the length of the tie rods are about 50 m. A structural steel of S275 grade has been used for all the components. Built-up members are characterized by the diagonals of two perpendicular planes welded in correspondence of the same cross-section of the chord. The angles between the tie-rods are 90° and between the tie-rods and the tower is 45°. Payload depends on boom inclination: in position (a), i.e. boom incline of 15° respect to the vertical axis, it is possible to reach the highest payload which must be decreased up to 1.25 times in the (b) position (boom inclined of 65° respect to the vertical axis) and up to 1.67 times in the (c) one (boom inclined of 80° respect to the vertical axis). Temperature, ice and seismic effects have not been considered in this paper. Due to the derrick geometry, both symmetric (SB in Figure 5) and non-symmetric (NS) configuration with respect to the horizontal plane have been considered: in SB cases boom is located at the bisector of the angle between tie-rods, while in NS cases boom is located near a tie-rod. For both configurations, three different values of boom inclination with respect to the vertical axis have been considered. In summary, the following geometries have been modelled:

- symmetric configuration on the horizontal plane (SB):
    - SB15: boom inclined of 15°;
    - SB65: boom inclined of 65°;
    - SB80: boom inclined of 80°;
- non-symmetric configuration on the horizontal plane (NS):
    - NS15: boom inclined of 15°;
    - NS65: boom inclined of 65°;
    - NS80: boom inclined of 80°.

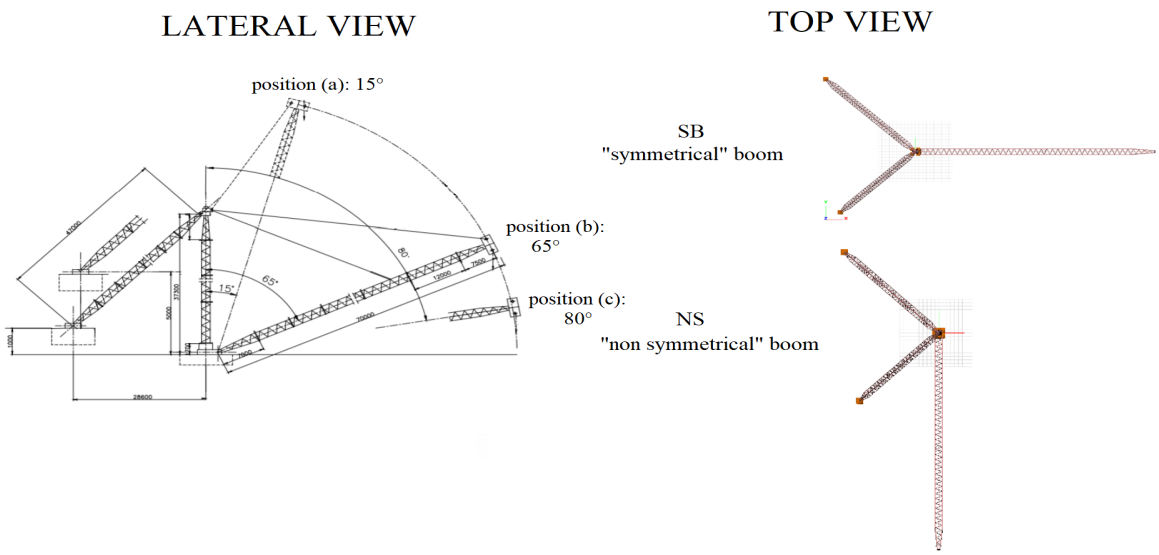

Figure 6: The considered derrick configurations

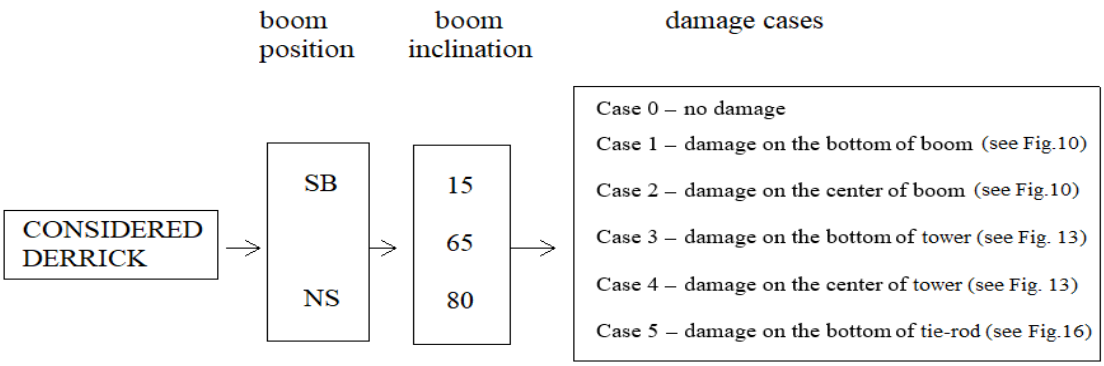

Figure 7: Layout of the considered design cases

In addition to initial cases (Case 0-no damage), five different removal scenarios were considered and Figure 6 presents the layout of all the considered numerical cases for a total of 30 design cases. As for the boom, reference is made to the removal of one element from the bottom (Case 1) or the center (Case 2). Furthermore, also for the tower, it has been supposed to be the lack of performance of one element of its bottom (Case 3) or its top (Case 4). Finally, Case 5 is related to the damage on one of the two tie-rods. All the derrick components (tower, boom, tie rods) have been modelled via beam elements without internal releases, due to the presence of welding. The top of the tower has been connected with tie-rods via a spherical hinge while at the base of both boom and tie rods, rotations are admitted only in one direction while all the translations are hampered. The base of the tower is perfectly fixed to the ground with an eccentricity from the base of the boom. Details of the model have been sketched in Figure 7. Resulting mesh is characterized by 2200 nodes and 360 FE beams for the boom, 121 for the tower and 630 for the two tie-rods. In the model each rope was modelled via 3 truss elements.

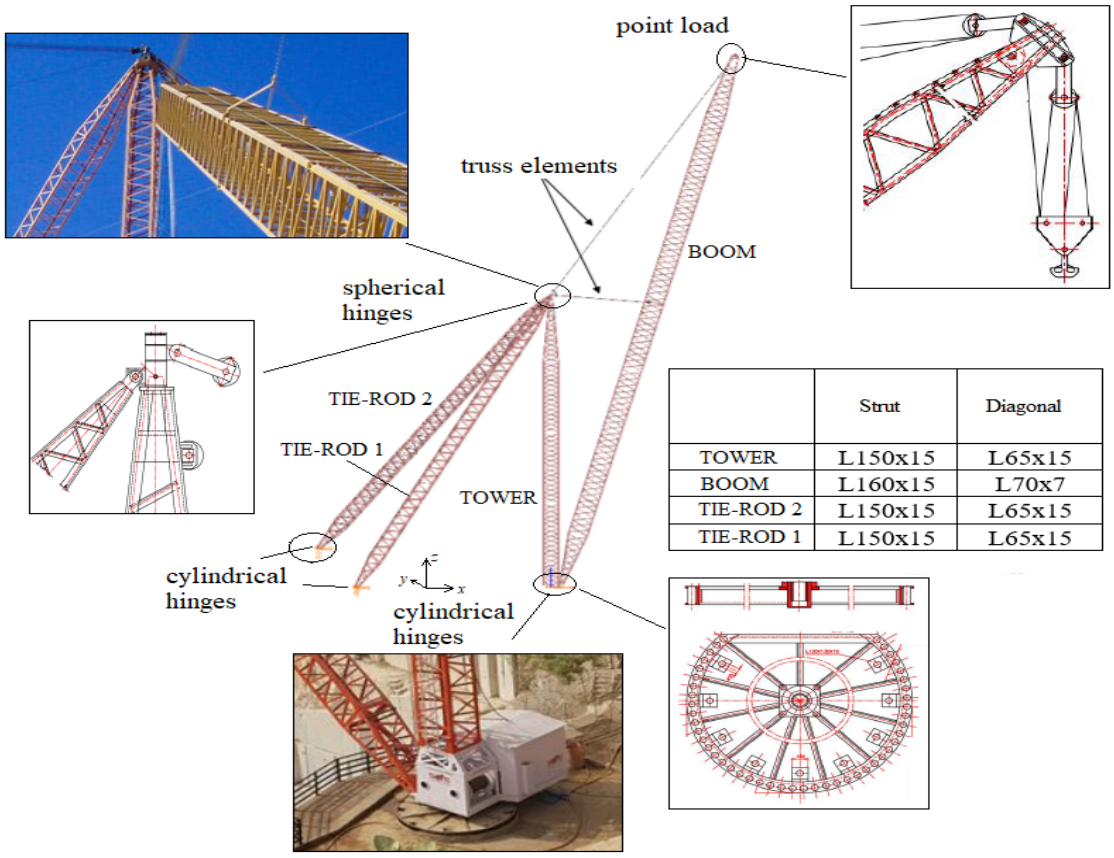

	Strut	Diagonal
TOWER	L150x15	L65x15
BOOM	L160x15	L70x7
TIE-ROD 2	L150x15	L65x15
TIE-ROD 1	L150x15	L65x15

Figure 8: Derrick details and cross-section data

Derrick static performance (Case 0)

As required by EC3-1-1 [22] and by other provisions dealing with structural steel design, overall buckling analyses have at first to be performed to appraise the buckling load multiplier (αcr) for each load combination of interest, in order to include/exclude the second order effects into design analysis. For the considered cases related to the undamaged derrick, the values of the buckling load multipliers are reported in Table 1, together with the description of the associated buckling modes. The three types of the overall buckling modes are depicted in Figure 8. Non-linear analyses by considering geometrical effects have hence always been performed, being αcr values (Table 1) lower than 10.

Table 1. Case 0: results from global buckling analysis α_{cr}

Derrick	Case 0
SB15	6.12 (boom translation)
SB65	4.61 (tower torsion)
SB80	4.59 (tower torsion)
NS15	6.05 (boom translation)
NS65	5.94 (rod2 torsion)
NS80	6.61 (rod2 torsion)

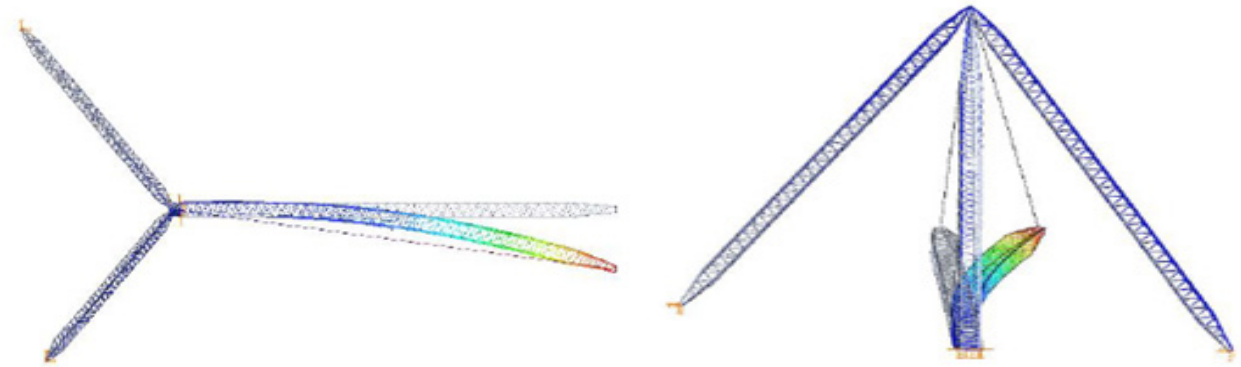

(a)

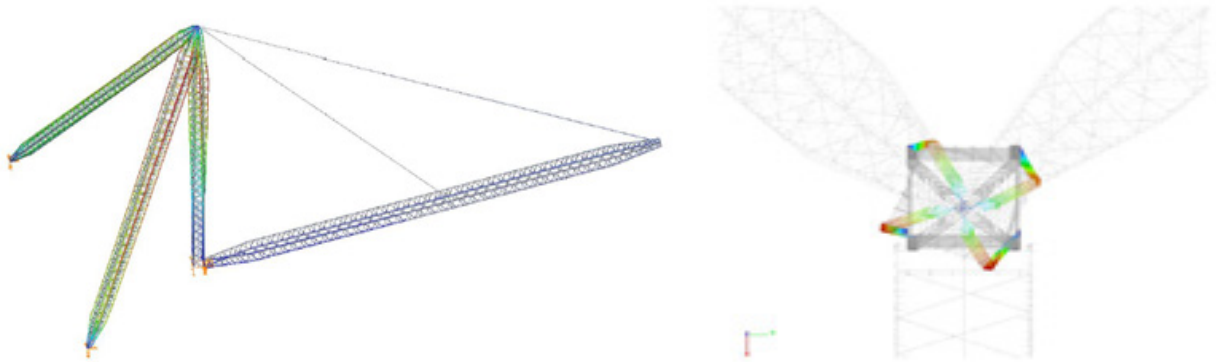

(b)

Figure 9: Overall buckling deformed shapes: boom translation (a) and torsion in tower (b)

For all members, safety factor (SI) has been calculated by using the GEM method, following the procedure previously discussed. In Table 2 the maximum (Max) and the average (mean) values of the SI obtained along all elements gained from the 7 DOF analyses have been presented, together with the standard deviation (dev) and the 95% fractile value (fract). Despite the fact that in all considered cases the maximum SI factor is close to the unity, i.e. no more load can be carried, all mean values are quite low (the highest is 0.52): this is due to a local increment of the SI in specific cross-sections caused by the presence of non-negligible bending moments and bimoment, which cannot be appraised via a traditional 6DOFs FE analysis leading for the same cases to values of SI always lower than unity [13]. Furthermore, the number of cross-sections for which the safety is not guaranteed via a 7DOFs design approach is quite limited, as it also appears from the low standard deviation and fractile values. The highest SI are located in the boom (SB15, NS15, SB65, NS65), in the tower (SB80) or in the tie-rod2 (NS80). In all cases, SI for struts are always greater than the ones evaluated in diagonals. With the assigned payloads, the considered derricks are always on the safe side with the maximum SI equal to unity.

Table 2: Key design data related to the Case 0

Elements		SB15	SB65	SB80	NS15	NS65	NS80
BOOM struts	mean	0.33	0.36	0.33	0.34	0.32	0.27
	Max	0.96	0.98	0.91	1.00	1.00	0.88
	dev	0.0892	0.0777	0.0654	0.0870	0.0888	0.0693
	fract	0.45	0.48	0.45	0.45	0.47	0.40
BOOM diagonals	mean	0.12	0.15	0.15	0.12	0.13	0.12
	Max	0.66	0.69	0.77	0.66	0.67	0.76
	Dev	0.0851	0.1099	0.1110	0.0858	0.0876	0.0819
	fract	0.21	0.29	0.29	0.21	0.25	0.23
TOWER struts	mean	0.20	0.52	0.51	0.09	0.25	0.26
	Max	0.27	1.03	0.98	0.16	0.50	0.60
	Dev	0.0083	0.1120	0.0755	0.0163	0.0297	0.0403
	fract	0.21	0.66	0.63	0.10	0.29	0.31
TOWER diagonals	mean	0.09	0.16	0.16	0.10	0.11	0.10
	Max	0.25	0.70	0.69	0.36	0.66	0.75
	Dev	0.0827	0.1198	0.1195	0.0889	0.0966	0.0950
	fract	0.18	0.29	0.29	0.19	0.20	0.19
TIE-ROD1 struts	mean	0.14	0.27	0.24	0.14	0.26	0.24
	Max	0.64	0.91	0.88	0.63	0.88	0.82
	Dev	0.0666	0.1157	0.1088	0.0667	0.1138	0.1071
	fract	0.20	0.48	0.37	0.21	0.48	0.42
TIE-ROD1 diagonals	mean	0.13	0.19	0.18	0.13	0.16	0.15
	Max	0.76	0.74	0.74	0.75	0.75	0.74
	Dev	0.0949	0.1417	0.1411	0.0955	0.1282	0.1193
	fract	0.25	0.43	0.39	0.26	0.41	0.39
TIE-ROD2 struts	mean	0.14	0.23	0.20	0.22	0.34	0.30
	Max	0.83	0.97	0.94	0.85	0.97	0.99
	Dev	0.0752	0.1155	0.1109	0.0908	0.0965	0.0916
	fract	0.23	0.41	0.43	0.32	0.50	0.45
TIE-ROD2 diagonals	mean	0.13	0.18	0.18	0.13	0.14	0.13
	Max	0.77	0.69	0.74	0.78	0.72	0.74
	Dev	0.0982	0.1315	0.1323	0.0962	0.1096	0.1063
	fract	0.24	0.39	0.43	0.22	0.29	0.27

ROBUSTNESS EVALUATION

As previously introduced, robustness is a desirable property of structural systems that mitigates their susceptibility to progressive collapse or disproportionate collapse. Generally, local damage or local collapse in a derrick crane could be caused by:

i. corrosion. As derricks may remain in-situ for 15-20 years with poor maintenance, spread of corrosion is a quite common problem, leading to a local failure of elements (Figure 9);

ii. reach of the maximum stability resistance. Due to many factors, overload might happen. SI of one element, in the loading phase, may also significantly overpass the unity, leading to an overall collapse, as highlighted in [10]. Furthermore, as it appears from [13], if a derrick is designed with a non-adequate software, generalized forces, displacements and the critical load multiplier can be remarkably wrong;

iii. local impact. Machinery impacts can happen only on tie-rods since the other parts of the derrick are away from operators and machines.

Figure 10: Corroded details of a derrick crane

To evaluate the Robustness, a direct approach was followed: i) identification of both the more stressed elements and the elements presenting the higher probability to be subjected to spread corrosion; ii) direct deletion of these elements from the original (undamaged) model. To present the procedure, 5 different scenarios were developed and discussed in the following.

Robustness for damages on the boom (Cases 1 and 2)

The first two cases are associated with damages on the boom. In Figure 10 it can be noted that:

- for Case 1, one strut was removed at the bottom of the boom, close to the supports, simulating the effect of a spread corrosion;
- for Case 2, the strut was removed from the center of the boom. In this position there is the maximum value of axial load and, consequently, damage can be related to the collapse of the most stressed element.

The results in terms of buckling load multiplier are reported in Table 3: for Case 1 great differences were detected, with reduction from 1.7 up to 2.9 times of αcr with respect to the undamaged derrick (Case 0); otherwise, the influence of the damage in the center of the boom (Case 2) is more limited, despite non negligible, with the ratio up to 1.6 (for 3 configurations is approximately equal to the unity).

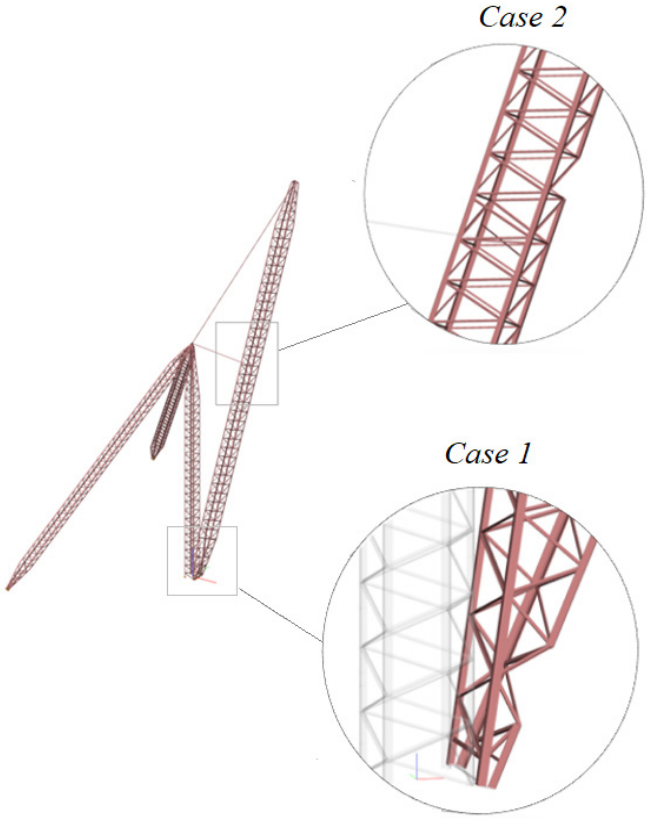

Figure 11: Cases 1 and 2: removal of one element from the bottom (1) or the center (2) of boom

As to the evaluation of the SI distribution in the built-up components, reference can be made to Figures 11 and 12, that, like the other ones associated with the other scenarios and discussed in the next sub-sections, are composed by three parts: one for the boom components, one for the tie-rods and one for the tower elements. In each of them, both diagonals and struts were considered. It is worth noting that the non-negligible differences in the elastic buckling of case 1 directly reflect an overall increase of all the SI. In Figure 11 the statistical

Table 3: Determination of the buckling multiplier α cr for Case 1 and Case 2

	Case 0	Case 1	Case 2	Case0/Case1	Case0/Case2
SB15	6.12 (boom flexure)	2.14 (boom flexure)	6.12 (boom flexure)	2.86	1.00
SB65	4.61 (tower torsion)	2.73 (tower torsion)	3.98 (tower torsion)	1.69	1.16
SB80	4.59 (tower torsion)	3.60 (tower torsion)	3.82 (tower torsion)	1.28	1.20
NS15	6.05 (boom flexure)	2.13 (boom flexure)	6.05 (boom flexure)	2.84	1.00
NS65	5.94 (rod2 torsion)	2.70 (rod2 torsion)	5.94 (rod2 torsion)	2.20	1.00
NS80	6.61 (rod2 torsion)	3.57 (rod2 torsion)	3.98 (rod2 torsion)	1.85	1.66

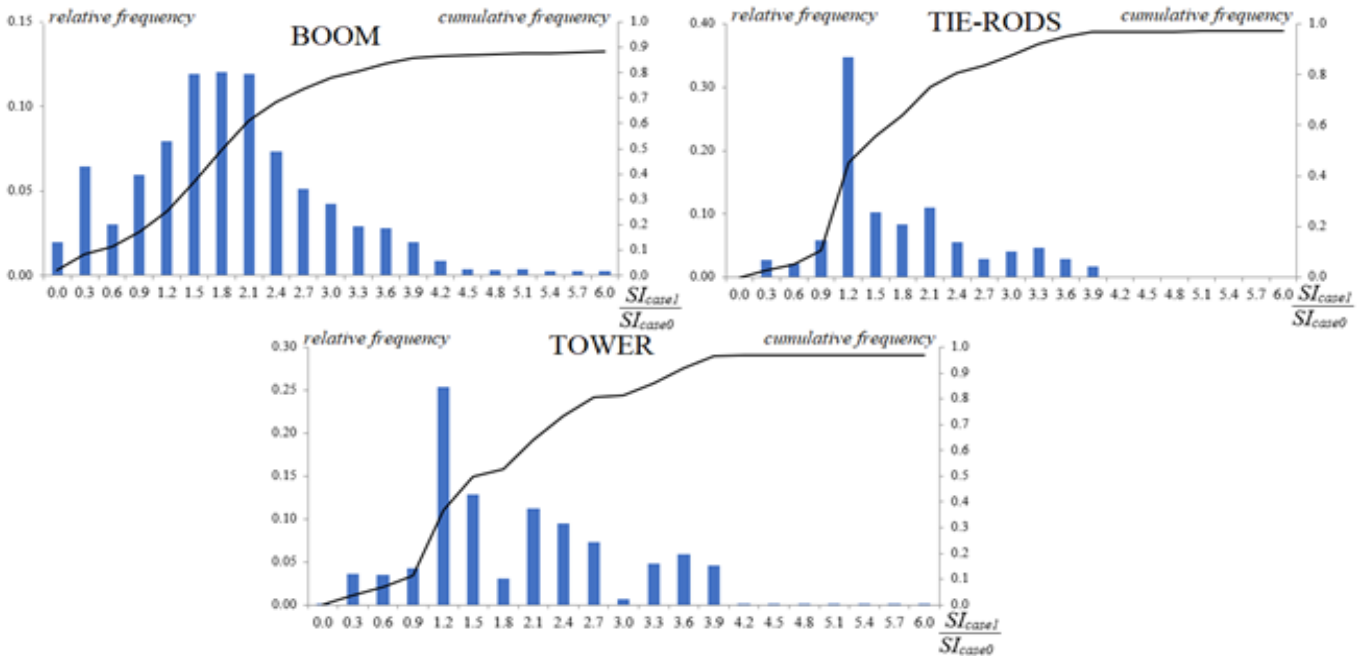

Figure 12: Distribution of the SIcase1/SIcase0 ratio for scenario 1

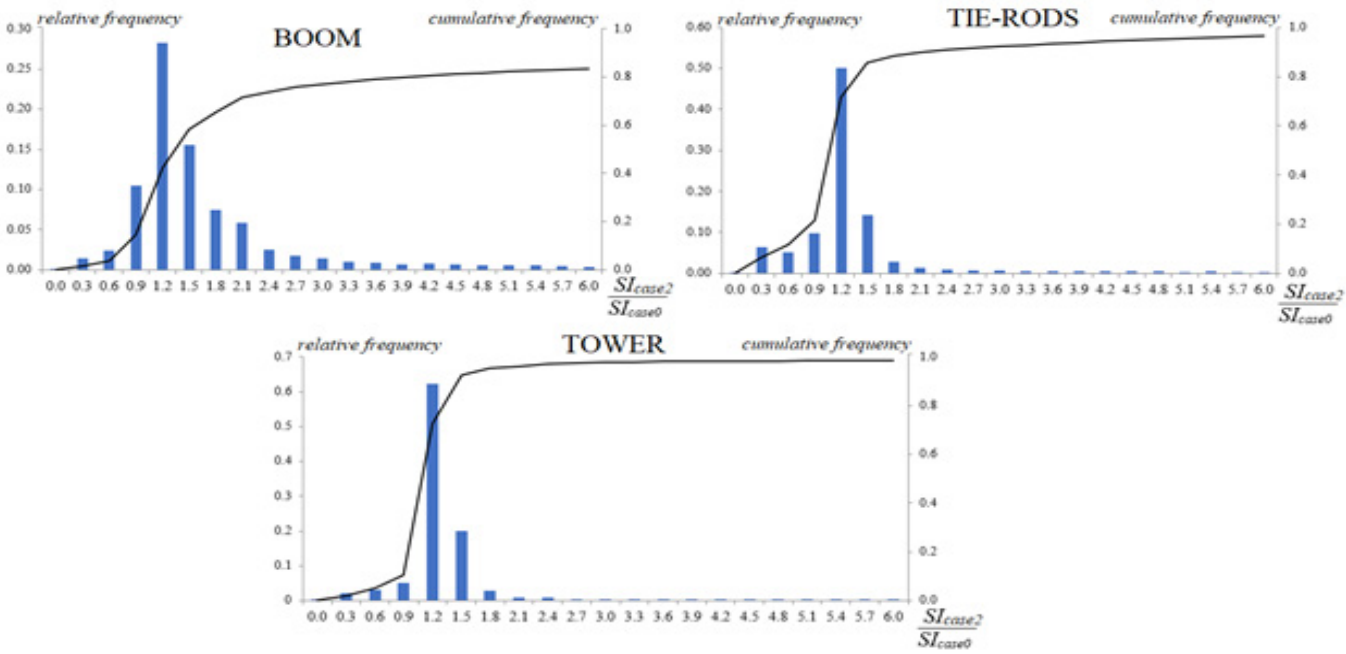

Figure 13: Distribution of the SIcase2/SIcase0 ratio for scenario 2

distribution of SIcase1/SIcase0 ratio has been plotted. The internal forces distribution remains quite similar to the undamaged cases with the only differences on the axial load distribution near to the damage zone on the bottom. For the Case 2 the second order analyses highlighted a different axial load distribution on the struts of the boom, increasing the values on the undamaged parts up to 50%. In the other components (tie-rods and tower) the values remain quite similar to the one associated with the undamaged cases. In Figure 12 the statistical distribution of SIcase2/SIcase0 ratio has been plotted. Furthermore, it can be noted that:

- some elements near to the removed one exhibited a change in stress state, passing from compression to tension. This directly reflects into SI ratios lower than unity;
- in all graphs, queues reach values up to 6. From an engineering point of view, these values are not relevant because related to SI much lower than unity;

- for the SIcase1/SIcase0 ratio, a huge number of values in boom are between 1.2 and 2.4. These values are mainly associated with SI factors that in Case 1 reach values over 2.0: this means that the applied load must be decreased. variation of the SI in tower and in tie-rod is limited. For both cases a great number of values are mainly in the range 0.90-1.20;
- for the SIcase2/SIcase0 ratio, for all the components, the change in the SI is quite negligible, all the values are mainly in the 0.9-1.2 range with the associated queues always negligible from an engineering standpoint.

It can be concluded that a damage in boom base elements (Case 1) greatly affects the behaviour of the whole structure for all considered configurations. From a purely mathematical point of view, all the configurations could carry a payload decreased up to 2 times with respect to the undamaged derrick. On the contrary, the damage in the middle length of the boom (Case 2) does not seem to significantly affect the derrick performance. However, in both situations, the machine should be immediately set in a safety condition (i.e., if possible lower lifted load) to put the derrick out of service. A repair intervention is required urgently before using the machinery again.

Robustness for damages on the tower (Cases 3 and 4)

Two damage scenarios for the tower (Figure 13) were considered, i.e.:

- Case 3, part of the strut is removed at the bottom of the tower simulating the effect of a spread corrosion;
- Case 4, part of the strut is removed at the top of the tower, close to the connection with the boom and the tie-rods. This position is extremely important because it is really hard to localize eventual damage here.

Results associated with analyses are reported in Table 4. For both the cases, differences with respect to the undamaged ones are generally quite low, up to 1.25 (Case 3) and 1.30 (Case 4). In Figures 14 and 15 the frequency distribution of ratio between SI evaluated and damaged and the one evaluated in the undamaged configurations are presented (SI_{case3}/SI_{case0} and SI_{case4}/SI_{case0}).

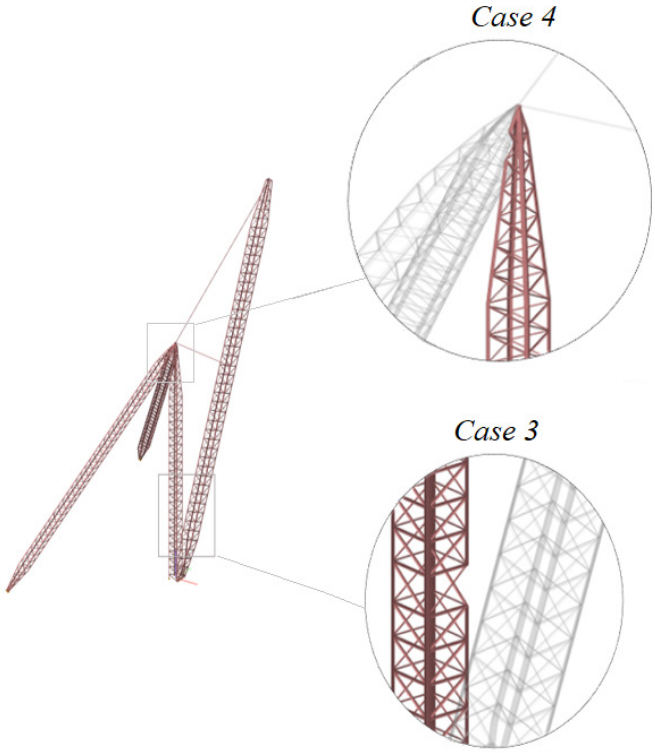

Figure 14: Cases 3 and 4: removal of one element from the bottom (3) and the top (4) of the tower

It can be noted that:

- also, for these cases, some elements near the removed ones exhibited a change in stress state, passing from compression to tension;

Table 4: Determination of the buckling multiplier α cr for Case 3 and Case 4

	Case 0	Case 3	Case 4	Case0/Case3	Case0/Case4
SB15	6.12 (boom flexure)	4.91 (boom flexure)	6.12 (boom flexure)	1.25	1.00
SB65	4.61 (tower torsion)	4.61 (tower torsion)	4.61 (tower torsion)	1.00	1.31
SB80	4.59 (tower torsion)	4.59 (tower torsion)	4.59 (tower torsion)	1.00	1.31
NS15	6.05 (boom flexure)	4.86 (boom flexure)	6.05 (boom flexure)	1.24	1.00
NS65	5.94 (rod2 torsion)	5.94 (rod2 torsion)	5.85 (rod2 torsion)	1.00	1.00
NS80	6.61 (rod2 torsion)	6.42 (rod2 torsion)	6.51 (rod2 torsion)	1.03	1.01

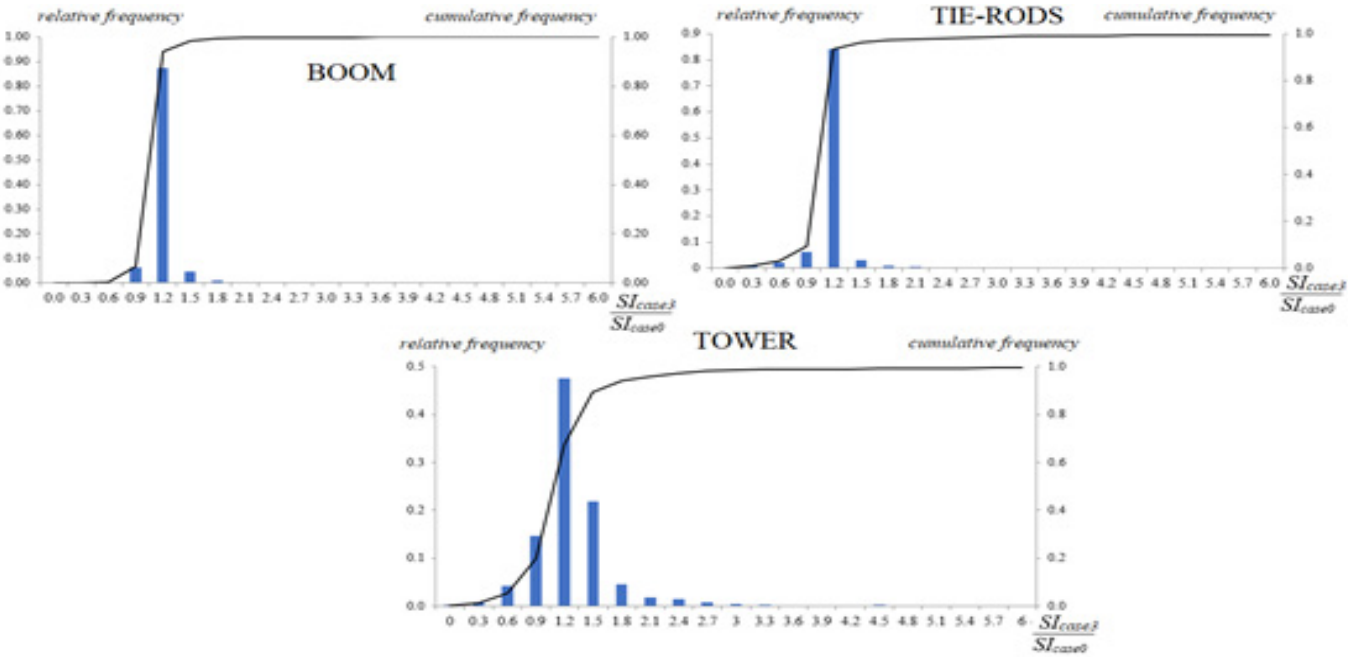

Figure 15: Distribution of the SIcase3/SIcase0 ratio for scenario 3

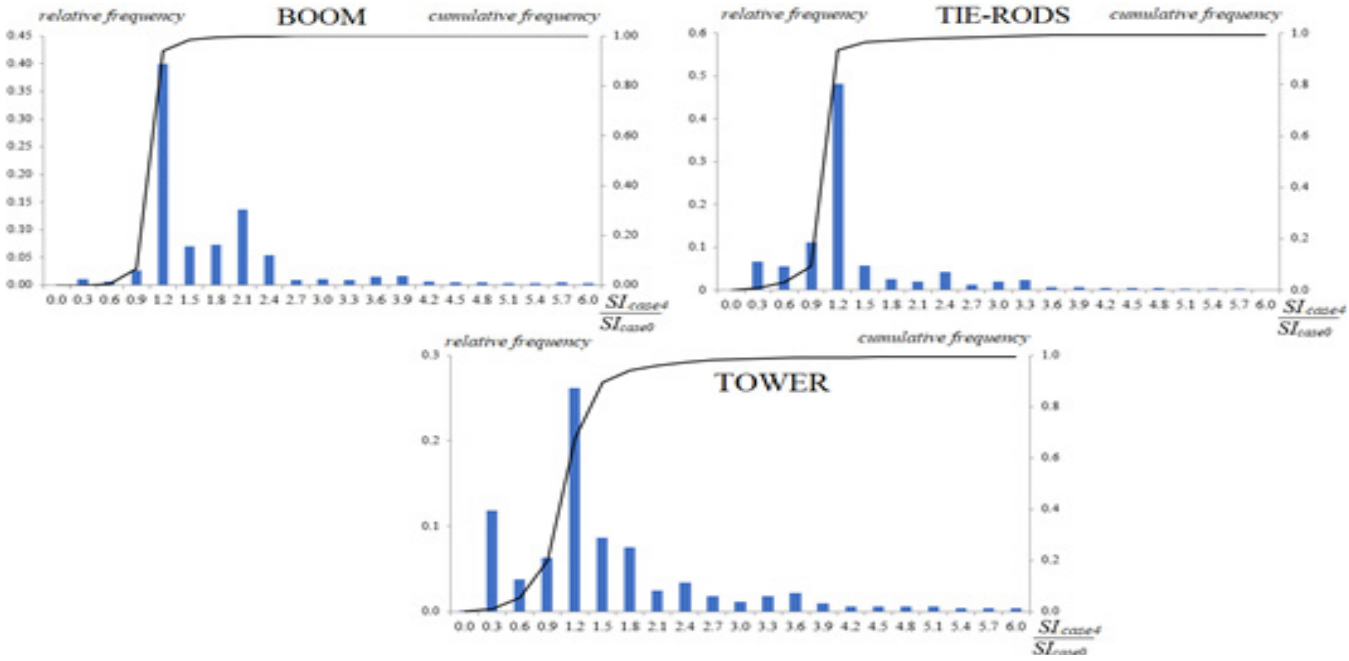

Figure 16: Distribution of the SIcase4/SIcase0 ratio for scenario 4

- if the results associated to the boom and to the tie-rods are considered, in both cases the values of ratios are mainly concentrated between 0.9-1.2, showing the little influence these damages have on the overall derrick behaviour;
- in the tower the variability of the SI ratio is important, with a great number of values comprised between 0.9 and 1.5;
- in both cases the queues are negligible.

For both the considered damages in the tower elements, the overall stability of the derricks is not greatly affected, maintaining the SI a little greater than the ones evaluated in undamaged configuration. From a purely mathematical point of view, all the configurations could carry a payload decreased up to 1.5 times with respect to the undamaged derrick. However, these considerations are valid only when the damage on the top of the tower does not also affect the global functionality of the derrick.

Finally, it can be concluded that also with these scenarios, the machine should be set in the safety condition and put derrick out of service. A repair intervention is always required.

Robustness for damages on tie-rod (Case 5)

As shown in Figure 16, for this case, a damage on one tie rod is considered. A damage in this point, is the only one that could be related to an accidental impact on tie-rod base.

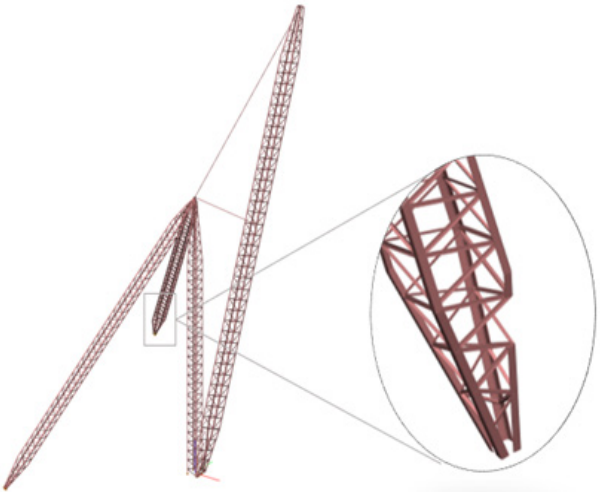

Figure 17: Case 5: damage on one tie-rod

Results of the buckling analyses are reported in Table 5. It can be noted that for all the considered cases the differences with respect to the undamaged derrick are always negligible, being less than 2%.

By considering Figure 17 reporting in terms of statistic distribution the SI_{case5}/SI_{case0} ratios, it can be noted that:

- in all of the graphs, values are mainly grouped in the 0.98-1.2 range. The queues are always related to SI values lower than unity, and hence not relevant from a designer standpoint;
- the most stressed cross-sections of Case 0 that reach the maximum SI, maintain the same value of SI also in Case 5, i.e. SI_{case5}/SI_{case0} ratio is equal to one.

In Case 5, the derrick still has the same stress distribution and stability condition with respect to the initial case. This damage does not greatly affect the derrick's global stability. However, also for this case a repair intervention is suggested since this typology of damage is the easiest to be identified in-situ.

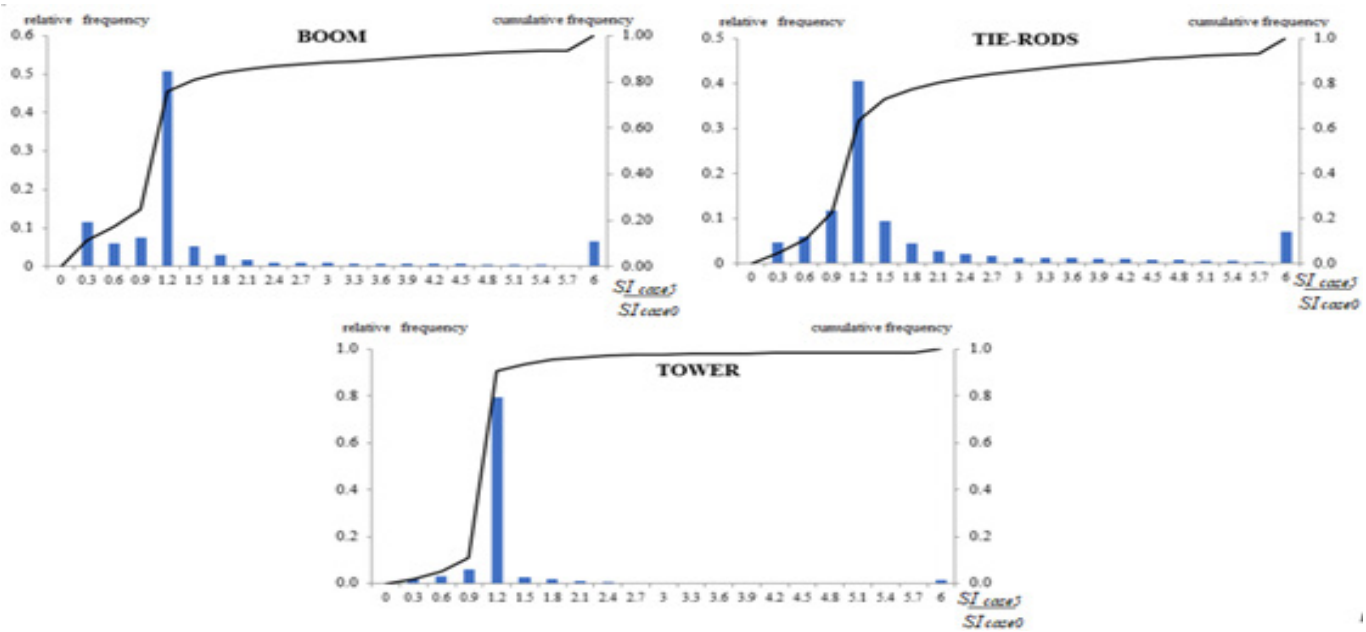

Figure 18: Distribution of the SI_{case5}/SI_{case0} ratio for scenario 5

Table 5: Determination of the buckling multiplier α cr, for Case 5

Derrick	Case 0	Case 5	Case0/Case5
SB15	6.12 (boom translation)	6.11 (boom translation)	1.00
SB65	4.61 (tower torsion)	4.61 (tower torsion)	1.00
SB80	4.59 (tower torsion)	4.59 (tower torsion)	1.00
NS15	6.05 (boom translation)	6.05 (boom translation)	1.00
NS65	5.94 (rod2 torsion)	5.84 (rod2 torsion)	1.02
NS80	6.61 (rod2 torsion)	6.51 (rod2 torsion)	1.02

CONCLUDING REMARKS

Steel angles are frequently used in built-up lattice members to realize lifting devices, such as overhead and gantry cranes, jibs of mobile cranes, portal cranes, tower and derricks cranes (which were considered in the present paper). The structural design of these machineries are usually carried out by simplified FEAPs offering the traditional 6DOFs beam formulation. Anyway, angles, channels, and other elements having a cross-section with a sole symmetry axis require for the structural analysis a more refined 7 DOFs beam formulation, i.e. the one solely able to account for the coupling between axial force and bending moments, as well as for the effects associated with warping torsion. The aim of the current research is to investigate the robustness of derricks, i.e. the sensitivity of these structures to local damages due to corrosion or loss of stability of some elements. Six different derrick configurations have been modeled by considering five different robustness scenarios (in addition to the undamaged one): damage on base (1) and center (2) of the boom, damage on bottom (3) and top (4) of the tower and damage on one of the tie-rods (5). For each scenario, buckling and second order analyses have been performed to evaluate the SI factor of all elements according to the EC3-GEM procedure. The comparison between all the results can be observed in Figure 18, where the SI_{casei}/SI_{case0} ratio for each i-th scenario is plotted. It can be concluded that:

- damages located at the boom (Cases 1 and 2) influence the overall behaviour greatly. In fact, if the damage is located at the bottom, the increment of the SI factor with respect to the initial case is mainly grouped within the range of 1.2-1.8 and the most influenced configurations are the ones with a boom inclination of 15°. On the contrary, when the damage is located in the center of the boom, the influence on the SI values is limited. For this case great variation can be observed only with respect to a boom inclination of 80°. Even if a derrick could be used in lifting a decreased payload, the machinery must be immediately put out of service in both cases;
- when the damage is located in the tower (Cases 3 and 4), its influence is always limited. The ratios between SI factors are always contained within the 0.9-1.2 range. Moreover, for damage at the bottom, the only case that shows big differences with respect to the undamaged one is the one with the boom in a symmetric position and an incline of 15°. When the damage is on the top of the two most stressed cases are the SB65 and SB80 ones, which are also the cases with the maximum values of the axial forces acting on the tower struts. Also for these cases, even if a derrick could be used in lifting a decreased payload, the machinery must be immediately put out of service in both cases;
- if the damage is located at the bottom of one tie-rod (Case 5), the stability of the whole derrick is not compromised, and the increment of SI factors is grouped mainly in an interval of 0.9-1.2. The derrick can be used with the same level of confidence of the initial case however a repair intervention must be performed.

Finally, it can be noted that this type of structures cannot be considered as Robust since at least one scenario has been found in which local damage generates disproportionate overall collapse.

ACKNOWLEDGMENTS

The authors would like to thank Consteel Company [19], who offered Consteel to the research group and to few students of the course of Steel Structures at the Politecnico di Milano (Italy).

REFERENCES

1. Shapiro, L. K., Shapiro, J. P. (2010). Cranes and derricks. McGraw-Hill Education, 4th edition. New-York. ISBN: 9780071625579 007162557.
2. UCIMU (2017). Guide to application of the Machinery Directive 2006/42/EC. Edizioni TNE, 2nd edition.

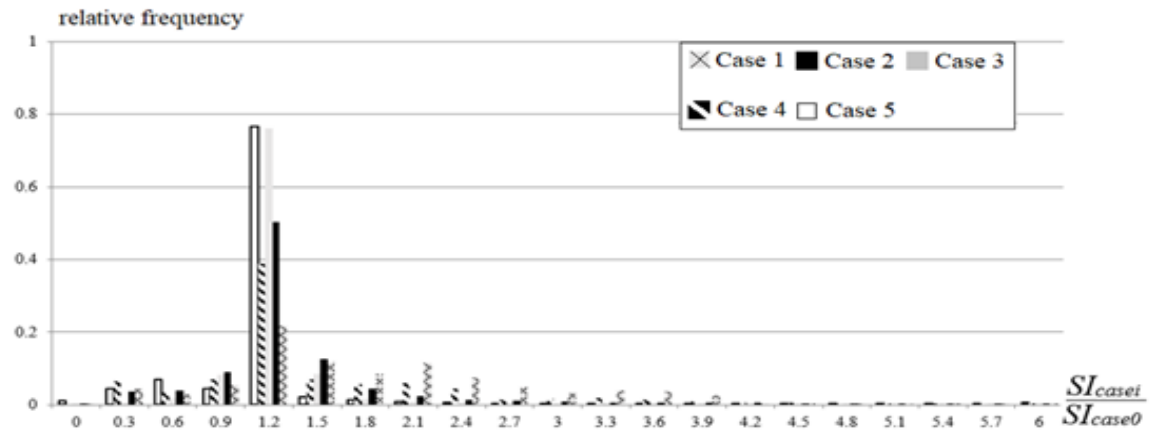

Figure 19: Distribution of the SI_{casei}/SI_{case0} for all the considered cases

3. Spasojevic-Brkic, V., Golubovic, T., Milanovic, D.D., Brkic, A. (2014). Crane operators anthropomeasures factors identification. Journal of Applied Engineering Science, vol. 12, no. 2, 159-164. doi: 10.5937/jaes12-5409.
4. Dondur, N., Spasojevic-Brkic, V., Brkic, A. (2012). Crane cabins with integrated visual systems for the detection and interpretation of environment – Economical appraisal. Journal of Applied Engineering Science, vol. 10, no. 4, 191-196. doi: 10.5937/jaes10-2516.
5. Feng, M., Xiao, H., Zhang, Z., Lu, S. (2010) Mechanical stress analysis of port crane based on the condition of temperature field. ICIMIA 2010, 2nd International conference on industrial mechatronics and automation, vol. 1, art. no. 5538057, 172-176. doi: 10.1109/ICINDMA.2010.5538057.
6. Cai, F., Wang, X., Liu, J., Zhao, F. (2014). Fatigue life analysis of crane K-Type welded joints based on non-linear cumulative damage theory. Journal of mechanical engineering, vol. 60, no. 2, 135-144. doi: 10.5545/sv-jme.2013.1368.
7. Lee, H. H. (1998). Modeling and control of three-dimensional overhead crane. Journal of dynamic systems, measurement and control, transactions of the ASME, vol. 120, no. 4, 471-476. doi: 10.1115/1.2801488.
8. Abdel-Rahman, E.M., Nayfehn, A.H., Masoud, Z.N. (2003). Dynamics and control of cranes: A review. JVC/Journal of vibration and control, vol. 9, no. 7, 863-908. doi: 10.1177/1077546303009007007.
9. Abdullahi, A.M., Mohamed, Z., Selamat, H., Pota, H.R., Zainal Abidin, M.S., Fasih, S.M. (2020). Efficient control of a 3D overhead crane with simultaneous payload hoisting and wind disturbance: design, simulation and experiment. Mechanical Systems and signal processing, vol. 145, 106893. doi: 10.1016/j.ymssp.2020.106893.
10. Solazzi, L. Zrnic, N. Design of a high-capacity derrick crane considering the effects induced by load application and release. Journal of Applied Engineering Science, vol. 15, no. 1, 409, 15-24, 2017. doi: 10.5937/jaes15-11930.
11. Solazzi, L. (2020). Effect of recurrent impulse load actions on a Crane. FME Transactions, vol. 48, no. 2, 266-271. doi: 10.5937/fme2002266S.
12. Solazzi, L., Scalmana, R. (2013). New design concept for lifting platform made of composite material. Applied composite materials, vol. 20, no. 4, 615-626. doi: 10.1007/s10443-012-9287-2.
13. Bernuzzi, C., Bertinotti, E., Simoncelli M. (2017). Structural analysis of built-up members with angles. Journal of Applied Engineering Science, vol. 18, no. 3, 443-457. doi: 10.5937/jaes18-24459.
14. Zandonini, R., Baldassino, N., Freddi, F. (2014). Robustness of steel-concrete flooring systems – An experimental assessment. Stahlbau, vol. 83, no. 9, 608-613. doi: 10.1002/STAB.201410192.
15. Diaz, E., Soria, L., Gallardo, J.M. (2019). Post-failure life evaluation: a corrosion-fatigue case history. Engineering failure analysis, vol. 105, 828-836. doi: 10.1016/j.engfailanal.2019.07.022.
16. DIN15018-1:1984 (1984). Cranes steel structures, Verification and analyses, Deutsche norm.
17. FEM 1.001 (1998), rules for the design of hosting appliances, federation europeene de la manutention, 1998.
18. EN13001-1 (2015), Cranes – General design – Part 1: General principles and requirements, Brusselles, 2015.
19. ConSteel v. 13, FE software, http://www.consteel-software.com/en, accessed 2019.
20. Vlasov, V. Z. (1961). Thin-walled elastic beams. Published for The National Science Foundation, Washington D.C., by the Israel Program for Scientific Translations, Jerusalem.
21. Bleich, F. (1952). Buckling strength of metal structures. Engineering societies monograph, McGraw Hill, New York. ISBN 10: 0070058903.
22. EN1993-1-1, Eurocodice 3 (2015), Design of steel structures – Part 1-1: General rules and rules for builsings, CEN.
23. Bernuzzi, C., Cordova, B., Simoncelli, M. (2015). Unbraced steel frame design according to EC3 and AISC provisions. Journal of Constructional Steel Research, vol. 114, 157-177, 4247. doi: 10.1016/j.jcsr.2015.07.012.

Paper submitted: 4.10.2021.
Paper accepted: 25.11.2021.
This is an open access article distributed under the CC BY 4.0 terms and conditions.